Coulombic and Hydrophobic Interactions in the First Intracellular Loop Are Vital for Bradykinin B2 Receptor Ligand Binding and Consequent Signal Transduction†

Jun Yu,‡ Peter Polgar,‡ David Lubinsky,‡ Megna Gupta,‡ Lei Wang,§ Dale Mierke,§ and Linda Taylor*,‡

Department of Biochemistry, Boston University School of Medicine, Boston, Massachusetts 02118, and Department of Molecular Pharmacology, Division of Biology and Medicine, and Department of Chemistry, Brown University, Providence, Rhode Island 02912

Received August 9, 2004; Revised Manuscript Received February 2, 2005

ABSTRACT: The role of the first intracellular loop (IC1) in the function of the rat bradykinin B2 receptor (BKB2R) was probed. On the basis of the bovine rhodopsin X-ray structure, the BKB2R IC1 consists of six residues: ^{60}HKTNCT. Exchange of this sequence with the bradykinin B1 receptor IC1 (PRRQLN) resulted in a chimera which bound bradykinin and signaled as wild-type (WT) BKB2R. In contrast, a chimera containing the IC1 of rat angiotensin II type Ia receptor (AT1aR) (YMKLKT) did not bind BK nor signal in response to BK at a concentration as high as 5 μM. ELISA illustrated that this receptor was still processed and inserted into the plasma membrane. Employing portions of the IC1, we observed that ^{60}HKT of BKB2R could be exchanged as a group with either the BKB1R (PRR) or AT1aR (YMK) with no change in receptor binding or signaling activities. When only the YM of AT1aR replaced the HK of BKB2R, leaving the N-terminal portion of IC1 without a positively charged residue, binding and signaling were reduced by more than 70%. When only N63 was replaced with the corresponding leucine of AT1aR, binding and signaling were ablated. In fact, replacement of the entire IC1 with the AT1aR except for N63 resulted in binding and signaling as WT BKB2R. However, N63 could be replaced by glutamine (in BKB1R) or aspartate and continued to function as WT BKB2R. NMR data indicated that the BKB2R IC1 extends beyond the bovine rhodopsin prototype to include HKTNCTVAEI. When E68 was exchanged with a serine (in AT1aR), ligand binding decreased by 60% and PI turnover decreased by 69%. Molecular modeling points to a strict requirement for a hydrophilic residue at position 63 (N) at the middle of the IC1 and a Coulombic charge interaction between the positive charges (H60 and K61) at the N-terminus and a negative charge (E68) at the C-terminus of the IC1.

The bradykinin B2 receptor (BKB2R)[1] is known to participate in a number of physiologic actions related to inflammation, pain, asthma, and blood vessel function (*1*). Often the physiologic role of the BKB2R opposes that of the angiotensin II type 1 receptor (AT1R) while working in cooperation with the bradykinin type B1 receptor (BKB1R). The biological function, cloning, and the various intracellular motifs participating in signaling and self-maintenance (internalization, desensitization, and resensitization) of the BKB2R have been reviewed recently (*2*−*5*). BKB2R is a constitutively expressed G-protein-coupled receptor (GPCR). It couples to $G_{q/11}$ as characterized by phospholipase C (PLC) activity and the turnover of phosphatidylinositol and to G_i as characterized by phospholipase A_2 (PLA_2) activity and the release of arachidonic acid (ARA) (*3*). The mobilization of Ca^{2+} is another characteristic of this receptor when activated through BK binding (*6*). The BKB2R also elicits responses that are not typically GPCR linked but are associated with the signal transductions of receptor tyrosine kinases and protein tyrosine phosphatases (*2*).

We have used receptor hybrid formation among the BKB2R, AT1aR, and BKB1R and point mutations to identify motifs participating in signaling and receptor maintenance and to address the molecular interplay among the multiple protein domains of the BKB2R (*7*). Whereas much has been reported as to the participation of the C-terminus and second and third intracellular loops in the function of this receptor, little is known as to the role of the first intracellular loop not only in BKB2R action but in the action of GPCR in general. In this report we construct chimeric mutants of various lengths between the IC1 of BKB2R and AT1aR or BKB1R. We observe that the IC1 acts as a determinant in ligand binding. When the entire IC1 of the BKB2R is exchanged with the IC1 of the AT1aR, the receptor loses its ability to bind BK. This is not the case with the introduction of the IC1 of BKB1R into BKB2R. This selective exchangeability can be attributed to an important Coulombic interaction within the IC1 of BKB2R, which is not present in the AT1aR, and a hydrophobic residue located at the apex of the ATa1R IC1, which is not tolerated within the BKB2R

† This work was supported in part by NIH, NHLBI, Grants HL25776 (P.P.) and GM 54082 (D.M.).

* To whom correspondence should be addressed. Tel: 617-638-4717. Fax: 617-638-5339. E-mail: taylorl@bu.edu.

‡ Boston University School of Medicine.

§ Brown University.

[1] Abbreviations: BK, bradykinin; BKB2R, bradykinin B2 receptor; BKB1R, bradykinin B1 receptor; AT1aR, angiotensin II type 1a receptor; GPCR, G-protein-coupled receptor; ARA, arachidonic acid; PI, phosphatidylinositol; IC, intracellular; TM, transmembrane; WT, wild type; MD, molecular dynamics.

10.1021/bi048288i CCC: $30.25
Published on Web 03/12/2005

IC1. Additional mutations in combination with receptor modeling and high-resolution NMR of a peptide corresponding to the IC1 loop of BKB2R further illustrate that prediction of a GPCR loop length in accordance with the bovine rhodopsin receptor model is not applicable to the BKB2R IC1, and this approach should be used with care. The conformational features of the IC1, as described here, allow us to relate the functional results onto a structural framework.

MATERIALS AND METHODS

Materials. [^{3}H]BK (78 Ci/mmol), myo[1,2-^{3}H]inositol (45−80 Ci/mmol), and [^{3}H]arachidonate (60−100 Ci/mmol) were obtained from NEN Life Science Products. Analytical grade Dowex-X8 (AG-1-X8, 100−200 mesh) was obtained from Bio-Rad (Hercules, CA). Restriction endonucleases were purchased from New England Biolabs (Beverly, MA). Oligonucleotides were synthesized by Invitrogen, Inc. (Carlsbad, CA). The QuickChange mutagenesis kit was obtained from Stratagene (La Jolla, CA). Anti-FLAG M2-peroxidase conjugate and TMB substrate were from Sigma. Rat-1 cells were obtained from Dr. Robert Weinberg (Whitehead Institute, MIT). All other reagents were from Sigma (St. Louis, MO) unless stated otherwise.

Construction of Chimeras. (A) Site-Directed Silent Mutagenesis. To facilitate swapping of the first intracellular loop of BKB2R with different sequences, a silent *Nhe*I restriction site was created at position 48 by the QuickChange site-directed mutagenesis kit (Stratagene). The oligonucleotides used to create silent mutations were as follows: sense strand, 5′ CTG GGT CCT CTT CCT GCT AGC CGC ACT GGA GAA CAT C 3′; antisense strand, 5′ GAT GTT CTC CAG TGC GGC TAG CAG GAA GAG GAC CCA G 3′. *Bgl*II is a convenient natural restriction enzyme located at position 68.

(B) Generation of Mutant Receptors. To construct IC1 chimeric mutants, the pBluescript−BKB2R cassette was digested with *Nhe*I and *Bgl*II. The corresponding sense and antisense oligonucleotides (synthesized by Invitrogen, Inc.) of the IC1 of interest were then annealed at equal molar ratio and ligated into the digested cassette vector. The mutants were confirmed by DNA sequencing. The *Xho*I−*Xba*I fragment containing the chimera receptor mutant was subcloned to the bicistronic mammalian expression vector, pCMin (*8*). All of the chimeric constructs were sequenced by an in-house facility using an automatic DNA sequencer. Pure plasmid DNA for transfection into mammalian cells was isolated with the Qiagen Plasmid Midi kit.

Cell Culture and Transfection. Rat-1 cells were grown in Dulbecco's modified Eagle's medium (DMEM), containing 5% fetal bovine serum supplemented with 50 units/mL penicillin and 50 μg/mL streptomycin at 37 °C in a humidified CO_2 (5%) incubator. HEK293 cells were grown in DMEM medium, containing 10% fetal bovine serum supplemented with 50 units/mL penicillin and 50 μg/mL streptomycin. CHO cells were grown in Ham's F12 media supplemented with 10% fetal bovine serum, 50 units/mL penicillin, and 50 μg/mL streptomycin.

HEK293 and CHO cells were transiently transfected using the Lipofectamine method in a 24-well plate (for binding assay or arachidonic acid release assay) or 12-well plate (for PI turnover assay) according to the protocol of the manufacturer (Invitrogen, Inc.). Stable transfections of Rat-1 cells were performed using the calcium phosphate method (ProFection Mammalian Transfection Systems, Promega, Inc.). Stable transfectants were selected in the presence of 0.5 mg/mL G418. The neomycin-resistant cell culture was then expanded and tested for the amount of specific binding to [^{3}H]BK.

Ligand Binding and Receptor Internalization. Ligand binding and internalization of the wild-type and mutated BKB2R in intact Rat-1 cells were carried out as described previously (*8*−*10*). Briefly, 80−100% confluent cell monolayers in 24-well plates (Costar, Cambridge, MA) were incubated in binding buffer containing various concentrations of [^{3}H]BK ranging from 0.08 to 20 nM in the absence (total binding) or presence of 100 nM BK (nonspecific binding) for 2 h at 4 °C. Cells were washed three times with ice-cold buffer and then solubilized with 0.2% SDS. Radioactivity was determined in a β counter after addition of 2 mL of Ecolite scintillation fluid. Equilibrium binding data (K_d and B_{max}) were analyzed by best fit to a single site model using the SigmaPlot 8 program (SPSS Inc.). All experiments were performed in triplicate, and the results were confirmed in at least two independent experiments. The curve was derived from one representative experiment.

Enzyme-Linked Immunoassay. Cells (CHO or HEK293) in 24-well plates were transfected with either a FLAG-tagged BKB2 receptor construct or a FLAG-tagged BK receptor mutant with the AT substitution in the first loop (the Ai1 mutant). Cells were also transfected with empty vector. Forty-eight hours after transfection, cells were washed with phosphate-buffered saline (PBS) and then fixed for 5 min at room temperature in 3% paraformaldehyde. Cells were washed three times with PBS and then blocked by incubation in 1% BSA in PBS for 45 min at room temperature. Blocking solution was removed, and anti-FLAG M2-peroxidase conjugate (Sigma) in 1% BSA/PBS was added. After 60 min at room temperature, wells were washed three times with PBS and then incubated with 200 μL of TMB substrate (Sigma). The reaction was stopped with HCl and then diluted in water (200 μL of the reaction in 800 μL of water) before being read in a Genesys spectrophotometer at 450 nm.

Phosphoinositide Turnover. Rat-1 cells were incubated with 1 μCi/mL myo[^{3}H]inositol in 1 mL of growth medium for 16−24 h. Ten minutes prior to ligand stimulation, cells were exposed to DMEM containing 20 mM $LiCl_2$ and 20 mM Hepes, pH 7.4. Cells were then exposed to different concentrations of bradykinin for 30 min at 37 °C, and the incubations were terminated by removal of the media and the addition of 0.5 mL of 10 mM ice-cold formic acid. The formic acid soluble material was then added to 10 mL of 5 mM sodium tetraborate for neutralization. Total [^{3}H]IPs were extracted using a Dowex AG-1-X8 formate resin in an anion-exchange column and eluted with 2 M ammonium formate, pH 5.0, as described (*10*). Following the addition of Ecolite scintillation fluid (ICN Biomedical, Inc., Aurora, OH), samples were counted for radioactivity in a liquid scintillation counter (Pharmacia Biotech Inc.). Data are representative of three separate experiments.

Release of Arachidonate. Rat-1 cells were prelabeled with [^{3}H]arachidonate (0.2 μCi/well) for 16 h as described

previously (*10*). Briefly, cells were washed with 500 μL of Dulbecco's medium containing 2 mg/mL bovine serum albumin (radioimmunoassay grade, Sigma). Cells were then incubated in the same medium with various concentrations of bradykinin for 20 min at 37 °C. Medium was removed and centrifuged at 800*g* for 2 min. Radioactivity in an aliquot of the medium was determined in a scintillation counter after addition of Ecolite scintillation fluid. Data are representative of three separate experiments.

Nuclear Magnetic Resonance. The peptide corresponding to the IC1 loop of BKB2R, BKB2R (55−75), was chemically synthesized on solid support and purified by reverse-phase HPLC. The peptide was characterized by mass spectrometry and NMR. All of the NMR spectra were acquired on a Bruker Avance 600 MHz with the sample dissolved in dimethyl sulfoxide. The amino acid spin systems were identified through total correlation spectroscopy (TOCSY) experiments, following previously published procedures (*11*). The sequential assignment and interproton distance restraints were obtained from NOESY spectra with a mixing time of 150 ms. The secondary shifts were calculated relative to the tabulated chemical shift values for Hα protons in random coil conformations and were averaged over three consecutive residues (*12*).

Molecular Modeling. The molecular model of the BKB2R was built as described previously (*9*, *10*, *13*). Briefly, the experimental data from the X-ray structure of bovine rhodopsin were used to generate the topological arrangement of the transmembrane helices, with the loops and termini added to complete the model. The structural features of the BKB2R IC2, as determined experimentally previously (*11*), and the IC1 were added to the model. The model of the receptor was refined using molecular dynamics (MD) simulations and energy minimizations using the GROMACS program, version 3.1 (*14*, *15*). A series of mutated receptors representing each of the chimeras were soaked in a three-phase solvent box composed of water and decane used to mimic the hydrophilic/hydrophobic, biphasic nature of the membrane as previously detailed (*13*). To equilibrate the solvent and optimize the solvent−protein interactions, an initial MD simulation of 10 ps was implemented, constraining all heavy atoms of the peptide to their initial positions with a force constant of 1000 kJ mol^{-1} nm^{-1}. Subsequently, molecular dynamic simulations were carried out for 300 ps at 300 K, with a time step of 2 fs and periodic boundary conditions.

Data Analysis. The K_d and B_{max} of bradykinin binding and the EC_{50} and E_{max} (maximal response) of concentration−effect curves were estimated using the SPSS Inc. SigmaPlot 8 Program Pharmacology Module. Statistical evaluation of the data was carried out using the Student *t*-test. Probability values of less than 0.05 were considered significant for PI turnover and arachidonic acid release and of 0.01 for receptor internalization.

RESULTS

Substitution of the IC1 of BKB2R with That of AT1aR or BKB1R. The transmembrane helical regions of bovine rhodopsin have been identified on the basis of its crystal structure (*16*). The putative first loops of BKB2R, AT1aR, and BKB1R were determined by aligning the amino acid sequences of these receptors with the bovine rhodopsin sequence using the ClustalW program. For mutant constructs, as shown in Figure 1a, the IC1 of BKB2R was replaced by its counterpart from AT1aR (Ai1) or BKB1R (B1i1). To determine the binding characteristics of these mutant receptors, Rat-1 cells were stably transfected with the cDNA constructs. The K_d and B_{max} of WT BKB2R and B1i1 proved very similar as shown in the binding curves of Figure 1b. However, the binding of the Ai1 chimera to BK was negligible. To illustrate procedural reproducibility, binding curves of WT receptor were determined three separate times. Results are illustrated as an insert in Figure 1b. The K_d and B_{max} values are shown in the table insert in Figure 1b. The three separate experiments illustrate reasonable reproducibility. PI turnover (Figure 1c) showed a pattern in agreement with the binding results. The B1i1 receptor produced IP with approximately the same pattern as WT BKB2R in response to an increasing concentration of BK with an EC_{50} for WT BKB2R at 0.5 nM and B1i1 at 0.4 nM. Turnover of PI by Ai1 was minimal (Figure 1c). Arachidonic acid release by these mutants, as shown in Figure 1d, was also affected similarly following exposure to BK.

Detection of Mutant Receptors at the Cell Surface. To determine whether the nonbinding receptor was efficiently trafficked and properly inserted to the plasma membrane, we performed ELISA. We utilized paraformaldehyde-fixed, nonpermeabilized cells. The FLAG epitope was fused in-frame at the amino terminus of both the WT BKB2R and the nonbinding Ai1 chimera. Both receptor cDNAs were transiently transfected into HEK293 and CHO cells. ELISA for FLAG antigen was performed on the attached, intact, transfected cells. Results are presented in Figure 2a. Both receptors, WT BKB2R and Ai1, were expressed equally at the cell surface of both HEK293 and CHO cells. We then investigated whether the binding of Ai1 was poor because of a decrease in its affinity for BK beyond measurable determinations with [^{3}H]BK. To assess this possibility, IP formation was measured in response to increasing concentrations of cold BK (0.1, 0.5, 1, and 5 μM), well above its normal EC_{50} of approximately 0.5 nM. As illustrated in Figure 2b, no PI turnover was detected with BK concentrations up to 5 μM.

Importance of Basic Residues in the N-Terminal Region of IC1. To refine the investigation of the role of specific sequence(s) within the IC1 of BKB2R, smaller chimeric receptors were constructed. As illustrated in Figure 3a, the first three amino acids at the N-terminus of the BKB2R IC1 (HKT) were exchanged with the corresponding residues of the AT1aR (YMK) or BKB1R (PRR). We also exchanged the first two residues of the BKB2R (HK) to YM of the AT1aR IC1 to create a mutant, HK2YM. This mutant contained no basic residues in the N-terminal portion of the IC1. The bradykinin binding capability of both the YMK and PRR chimeras proved similar to WT BKB2R (Figure 3b). However, the mutant HK2YM displayed a normal K_d of 1.5 nM but a low B_{max}, only about 25% of the WT receptor. YMK and PRR chimera receptors displayed PI turnover and arachidonic acid release as WT BKB2R (Figure 3c). The HK2YM mutant exhibited very poor signaling capacity compared to WT. The EC_{50} value of 0.5 nM was retained for PI turnover, but the E_{max} was approximately 30%

a

```
WT    60HKTNCT
Ai1    YMKLKT
B1i1   PRRQLN
```

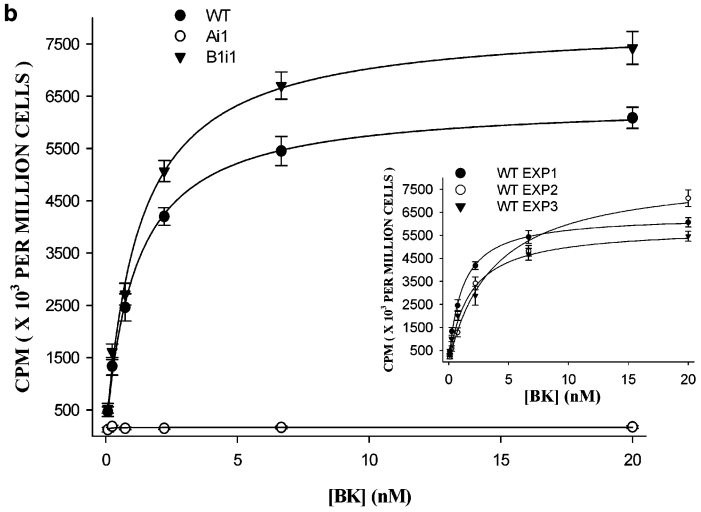

	Kd (nM)	Bmax (x 10^3 receptors per cell)
WT Exp1	1.1 ± 0.1	54.1 ± 1.5
WT Exp2	3.7 ± 0.6	69.8 ± 3.6
WT Exp3	1.7 ± 0.3	49.7 ± 2.5
Ai1	N.D.	1.4 ± 0.1
B1i1	1.2 ± 0.1	66.9 ± 1.8

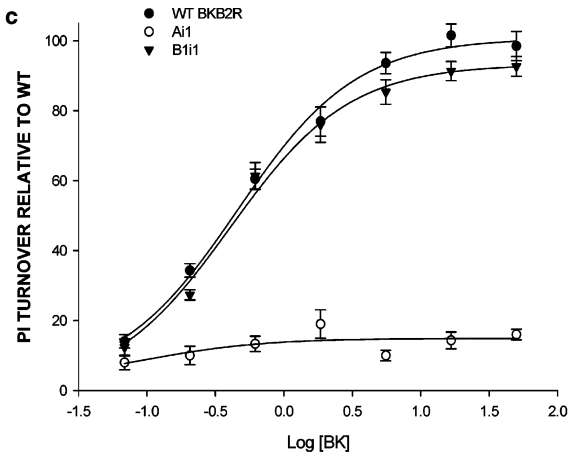

	EC50 (nM)	Emax (% of WT Emax)
WT B2R	0.5 ± 0.1	100.0 ± 2.1
Ai1	N.D.	14.9 ± 1.5
B1i1	0.4 ± 0.1	93.2 ± 2.2

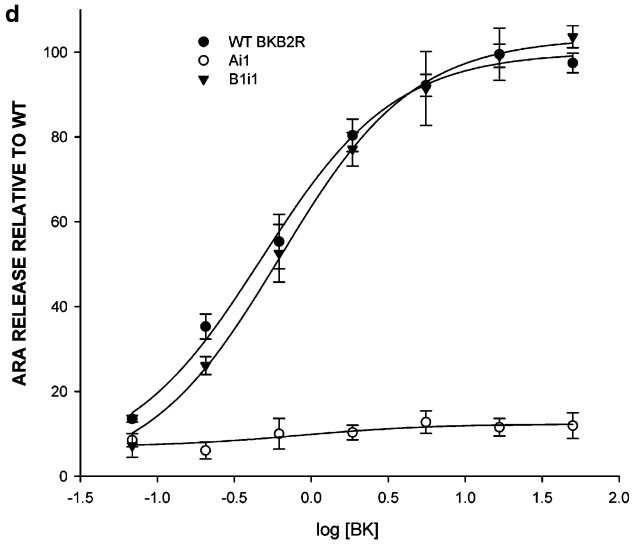

	EC50 (nM)	Emax (% of WT Emax)
WT B2R	0.5 ± 0.1	100.0 ± 2.5
Ai1	N.D.	12.8 ± 1.7
B1i1	0.6 ± 0.2	103.4 ± 3.1

FIGURE 1: Replacement of the IC1 of BKB2R with that of AT1aR or BKB1R. (a) Amino acid sequences of the IC1 of WT BKB2R and of the chimeras. Ai1: IC1 of the BKB2R substituted with that of AT1aR. B1i1: IC1 of the BKB2R substituted with that of BKB1R. (b) Ligand binding of the WT BKB2R and chimeric receptors. Ligand binding experiments were carried out using [^{3}H]BK on Rat-1 cells expressing WT or mutated BKB2R at concentrations ranging from 0.08 to 20 nM. The K_d and B_{max} of bradykinin binding were calculated using the SigmaPlot 8 Program Pharmacology Module (SPSS Inc.). B_{max} of the mutant receptor is presented as receptor sites per million cells. ND = not determined = value could not be calculated from nonlinear regression curve fit. Data are representative of at least two separate experiments. Inset: The binding curves of WT BKB2R carried out three separate times to illustrate reproducibility. The K_d and B_{max} are shown in the table within panel b. (c) Concentration−response curve of BK-stimulated inositol phosphate production in Rat-1 cells expressing WT BKB2R and IC1 chimeras. PI turnover was measured in myo[^{3}H]inositol-labeled cells as described in Materials and Methods. Results are presented as bradykinin-stimulated PI turnover minus basal IP normalized to that of WT. Each point is the average of cells from triplicate wells ± SE from a representative experiment of three experiments. The EC_{50} and E_{max} (maximal response) of PI turnover were calculated using the SigmaPlot 8 Program Pharmacology Module (SPSS Inc.). The E_{max} of each mutant receptor is represented as the percent of the PI turnover of WT BKB2R. ND = not determined = value could not be calculated from nonlinear regression curve fit. (d) Concentration−response curve of BK-stimulated ARA release in Rat-1 cells expressing WT BKB2R and IC1 chimeras. ARA release was measured in [^{3}H]arachidonate-labeled cells as described in Materials and Methods. Results are presented as bradykinin-stimulated ARA release minus basal ARA normalized to that of WT. Each point is the average of cells from triplicate wells ± SE from a representative experiment of three experiments. The EC_{50} and E_{max} (maximal response) of arachidonic acid release were calculated using the SigmaPlot 8 Program Pharmacology Module (SPSS Inc.). The E_{max} of each mutant receptor is represented as the percent of arachidonic acid release of WT BKB2R. ND = not determined = value could not be calculated from nonlinear regression curve fit.

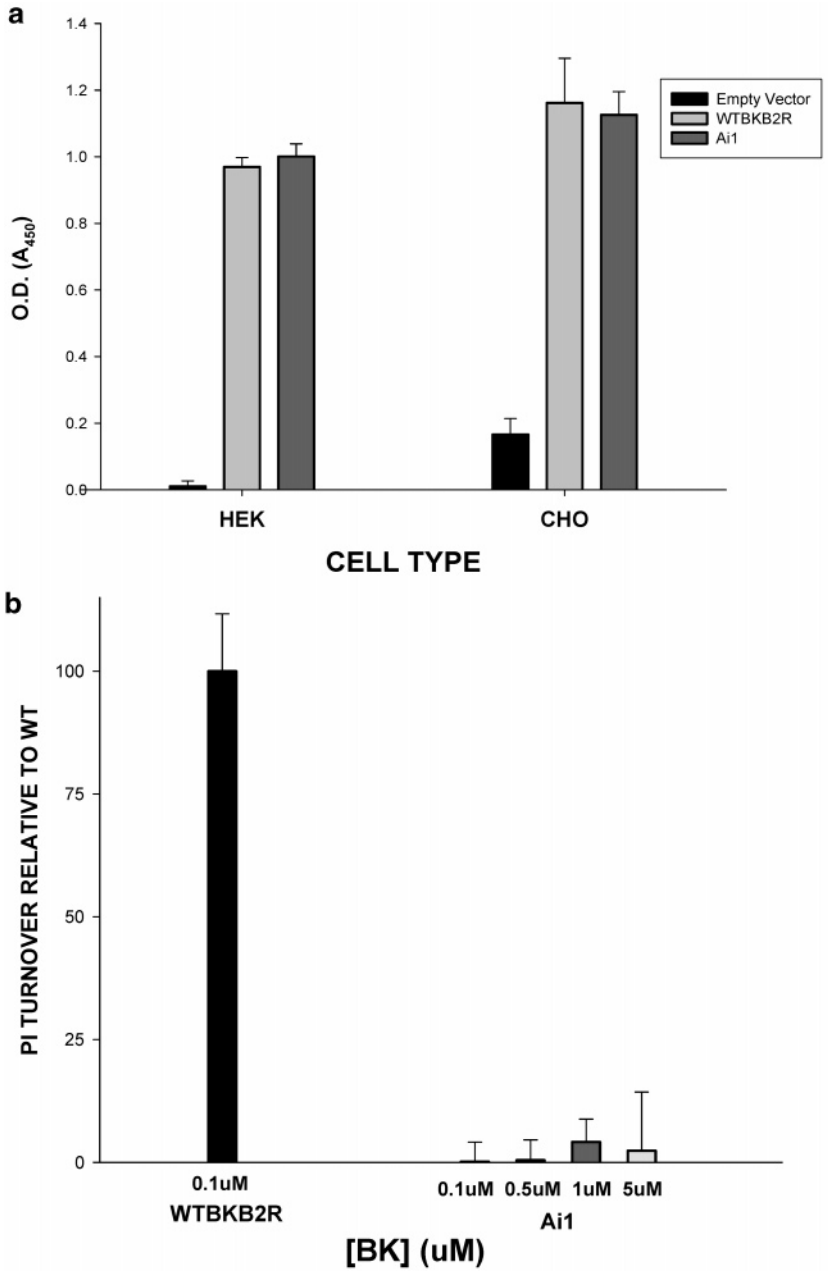

FIGURE 2: (a) ELISA. CHO and HEK cells were transiently transfected with FLAG-tagged WT BKB2R, FLAG-tagged Ai1 mutant, or empty vector. ELISA was performed as described in Materials and Methods. Error bars are mean ± SE obtained from three independent transfections. The experiment shown is representative of three experiments. (b) PI turnover response of WT BKB2R and Ai1 receptors at high concentrations of BK. PI turnover was measured in myo[^{3}H]inositol-labeled cells after stimulation with different concentrations of bradykinin (100, 500, 1000, and 5000 nM). Results are presented as percent of WT BKB2R.

of WT (Figure 3c). With respect to ARA release the EC_{50} was not determinable with reproducible accuracy while the E_{max} was 21% of WT (Figure 3d).

N63 Is Crucial for the Integrity and Function of BKB2R. Both AT1aR and BKB2R contain a threonine as their terminal IC1 amino acid. However, N63 and C64 are unique to the BKB2R (Figure 1a). The importance of N63 and C64 within the C-terminal portion of the IC1 of BKB2R was tested by rescue studies. Using the Ai1 mutant receptor, L63 was first replaced with the corresponding asparagine (N) of BKB2R (L63N, Figure 4a). Switching this one residue rescued the nonfunctional Ai1 to approximate the WT BKB2R both in ligand binding and receptor signaling, as determined by PI turnover and ARA release (Figure 4b−d). However, changing K64 in the nonfunctional Ai1 back to C (K64C, Figure 4a) failed to rescue Ai1. This mutant showed negligible ligand binding (Figure 4b) as well as poor PI turnover and ARA release (Figure 4c,d). These results demonstrate that N63 is crucial for the integrity and function of BKB2R.

A Hydrophobic Residue in Position 63 Is Deleterious. The deleterious effect of a hydrophobic residue in position 63 of the BKB2R was underscored by substitution of N63 in WT BKB2R to L (N63L, Figure 5). The B_{max} of this mutant was approximately 20% of WT. N63 substituted with either the amide, glutamine (Q, found in the same position in BKB1R), or a negatively charged residue, aspartic acid (D), bound BK as WT BKB2R, as illustrated in the same figure. Figure 5 also illustrates that C64 is not important for the binding efficiency of the receptor. Mutation of WT BKB2R C64 to

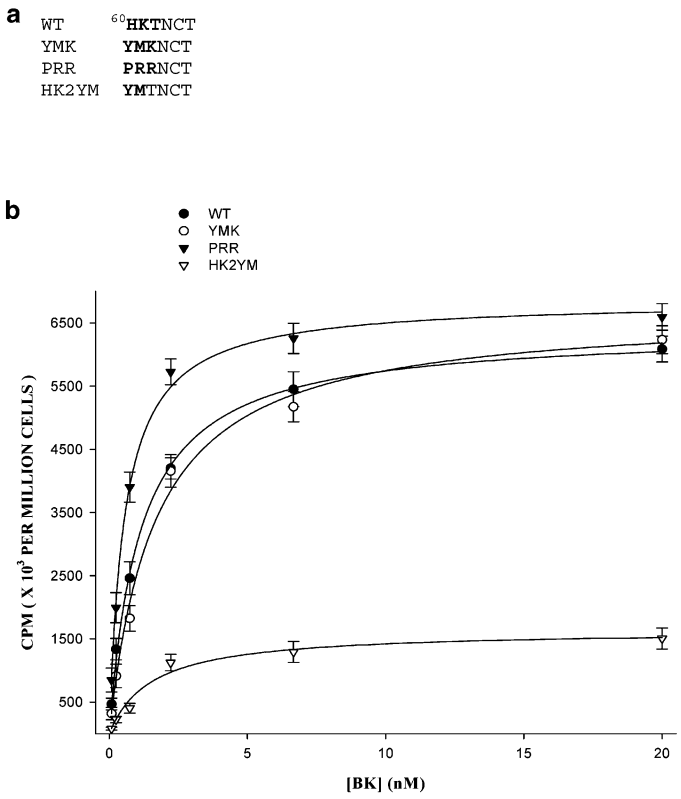

	Kd (nM)	Bmax (X 10^3 receptors per cell)
WT B2R	1.1 ± 0.1	54.1 ± 1.5
YMK	1.7 ± 0. 2	56.9 ± 2.0
PRR	0.6 ± 0. 1	58.3 ± 1.4
HK2YM	1.5 ± 0. 4	13.9 ± 1.0

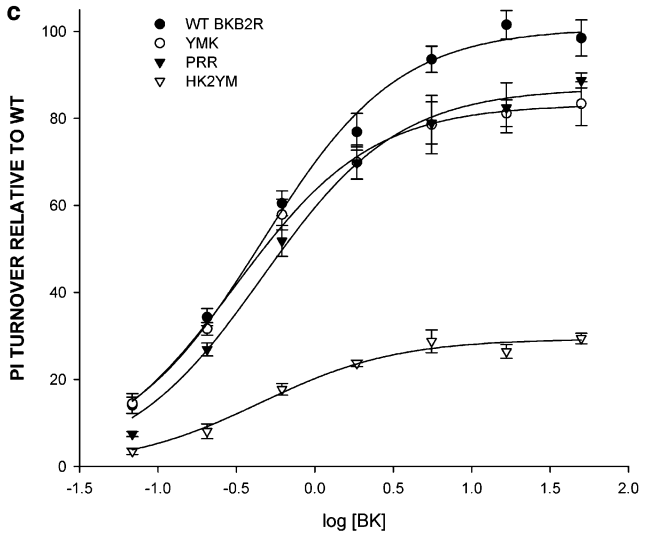

	EC50 (nM)	Emax (% of WT Emax)
WT B2R	0.5 ± 0.1	100 ± 2.1
YMK	0.3 ± 0.1	83.2 ± 2.3
PRR	0.5 ± 0.1	87.0 ± 2.3
HK2YM	0.5 ± 0. 2	29.3 ± 1.1

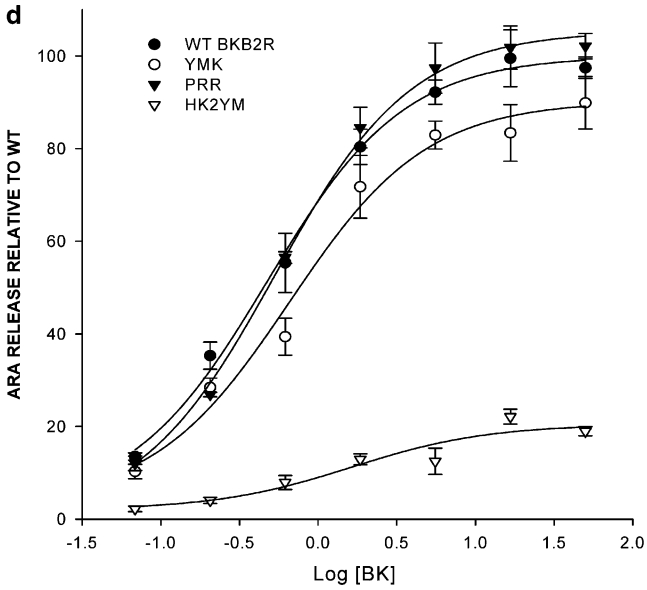

	EC50 (nM)	Emax (% of WT Emax)
WT B2R	0.5 ± 0.1	100.0 ± 2.5
YMK	0.7 ± 0.3	90.3 ± 3.3
PRR	0.5 ± 0.1	105.4 ± 2.2
HK2YM	N.D.	20.5 ± 1.6

FIGURE 3: Chimeric studies on the first three amino acids of BKB2R IC1. (a) IC1 sequence (exchange chimeras of the first three IC1 amino acids). YMK, first three amino acids of BKB2R IC1 changed to YMK in AT1aR; PRR, first three amino acids of BKB2R IC1 changed to PRR in BKB1R; HK2YM, first two amino acids (HK) of BKB2R IC1 changed to YM in AT1aR. (b) Ligand binding of the WT BKB2R and mutant receptors. Experimental procedures were the same as those described in Figure 1b. (c) Concentration−response curve of BK-stimulated inositol phosphate production. Experimental procedures were the same as those described in Figure 1c. (d) Concentration−response curve of BK-stimulated ARA release. Experimental procedures were the same as those described in Figure 1d.

a positively charged K (C64K), the counterpart residue in AT1aR, did not alter the binding of BK.

Experimental Examination of the IC1 Length. By using high-resolution NMR and a peptide construct containing this IC1 plus seven residues of the adjacent TM1 and TM2, we proceeded to experimentally determine the assignment of the IC1 of BKB2R. As shown in Figure 6, the secondary shift values of the Hα resonances (values more negative than 0.1 are consistent with α-helices) clearly indicate an N-terminal helix, corresponding to the end of TM1 at L59, and a

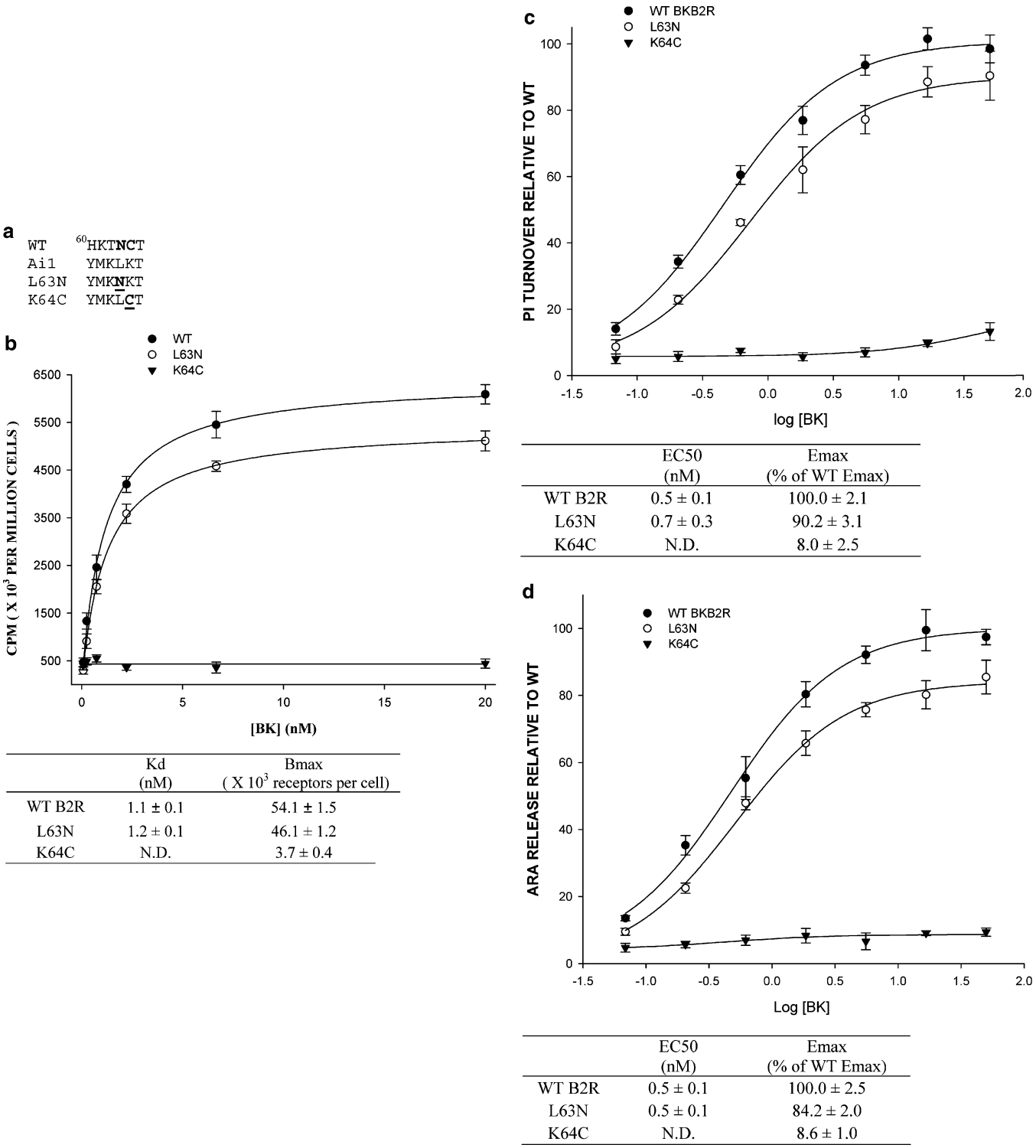

	Kd (nM)	Bmax (X 10^3 receptors per cell)
WT B2R	1.1 ± 0.1	54.1 ± 1.5
L63N	1.2 ± 0.1	46.1 ± 1.2
K64C	N.D.	3.7 ± 0.4

	EC50 (nM)	Emax (% of WT Emax)
WT B2R	0.5 ± 0.1	100.0 ± 2.1
L63N	0.7 ± 0.3	90.2 ± 3.1
K64C	N.D.	8.0 ± 2.5

	EC50 (nM)	Emax (% of WT Emax)
WT B2R	0.5 ± 0.1	100.0 ± 2.5
L63N	0.5 ± 0.1	84.2 ± 2.0
K64C	N.D.	8.6 ± 1.0

FIGURE 4: Mutagenesis studies on N63 and C64 of BKB2R. (a) Rescue constructs: L63N, L63 in mutant Ai1 was mutated back to the N in BKB2R; K64C, K64 in mutant Ai1 was mutated back to the C in BKB2R. For clarity, the amino acid sequences of this region in BKB2R and Ai1 are shown. (b) Ligand binding of the WT BKB2R and mutated receptors. Experimental procedures were the same as those described in Figure 1b. (c) Concentration−response curve of BK-stimulated inositol phosphate. Experimental procedures were the same as those described in Figure 1c. (d) Concentration−response curve of BK-stimulated ARA release. Experimental procedures were the same as those described in Figure 1d.

C-terminal helix, corresponding to TM2 starting at Y70. Therefore, NMR assigns the IC1 region starting at H60 and ending at I69. The sample was not soluble in any membrane mimetic (e.g., dodecylphosphocholine, sodium dodecyl sulfate, dihexylphosphocholine). The NMR studies were conducted in DMSO, a commonly used solvent.

The Importance of E68. In contrast to the projection by a strict adherence to the bovine rhodopsin X-ray crystal structure model, the NMR results assigned the IC1 of BKB2R from H60 to I69. On the basis of the sequence alignment between BKB2R and AT1aR, V65 and A66 are conserved in both receptors, and at position 69, BKB2R is

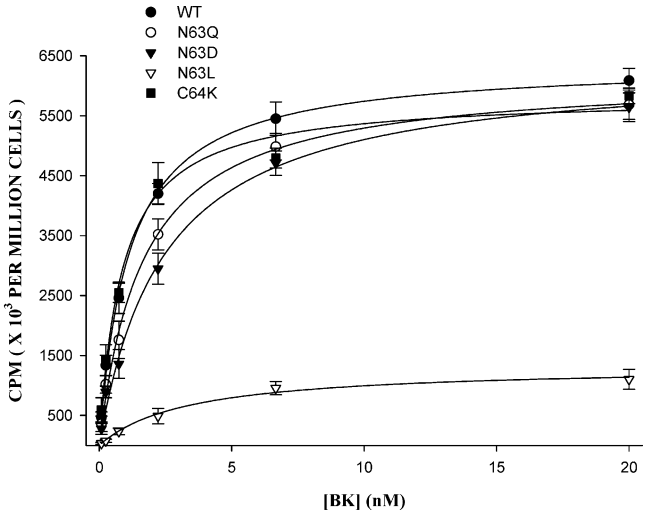

	Kd (nM)	Bmax (X 10^3 receptors per cell)
WT B2R	1.1 ± 0.1	54.1 ± 1.5
N63Q	1.7 ± 0.2	52.5 ± 2.0
N63D	2.5 ± 0.3	54.0 ± 2.2
N63L	3.4 ± 1.1	11.3 ± 1.2
C64K	0.9 ± 0.1	49.6 ± 1.8

FIGURE 5: Ligand binding of N63 and C64 point mutations: N63D, N63Q, and N63L, N^{63} of wild-type BKB2R was mutated to D, Q, or L, respectively; $C^{64}K$, C64 of WT BKB2R was mutated to K. The procedure for ligand binding is described in the legend for Figure 1b.

I, which is very similar to the corresponding V in AT1aR. However, position 68 is very different; there is an E in B2R, which is an acid residue, whereas an S in AT1aR lacks charge. To test the role of E68 in the BKB2R biologically, the residue was mutated to serine. The resulting mutant (E68S) showed only a 40% B_{max} compared to WT BKB2R. The K_d of this mutant remained normal (Figure 7a). At the same time, the PI turnover and arachidonic acid release of E68S were greatly impaired (Figure 7b,c). These results confirm that E68 plays an important role in the tertiary structure and signaling function of the BKB2R.

Molecular Modeling. Employing the previously established model of BKB2R (*3*, *9*), extensive molecular modeling and MD simulations were carried out to determine the location of the positively charged N-terminal end of the IC1 containing the residues HK in the BKB2R with respect to the negative E68 at the C-terminal end of IC1. As illustrated in Figure 8, the three residues in the N-terminal portion of the IC1 are in close proximity to the negatively charged E68. The N63 is located at the apex of the loop, fully solvated in the aqueous phase of the simulation cell.

Receptor Internalization. As illustrated in Figure 9, none of the mutations or exchanges with either the AT1aR or BKB1R affected endocytosis of the BKB2R mutants. No mutant uptake varied by more than 10% over 1 h following activation of the receptor with 100 nM BK. The *p* values for all mutant receptor uptake compared to WT BKB2R were well above 0.01.

DISCUSSION

Few reports have been published on the IC1 in GPCR in general. For example, some specific residues in the IC1 of cholecystokinin-A and -B receptors were identified as crucial for Gs coupling (*19*, *20*). Mutagenesis studies in gonadotropin-releasing hormone (GnRH) receptor also showed that cAMP signaling is dependent on residues in the IC1 that are not essential for activation of the phosphoinositide signaling pathway (*21*). Mutations of the IC1 of rhodopsin were shown to affect transducin activation leading to autosomal dominant retinitis pigmentosa (*22*). Thus far, only one study has been published on the IC1 of BKB2R.

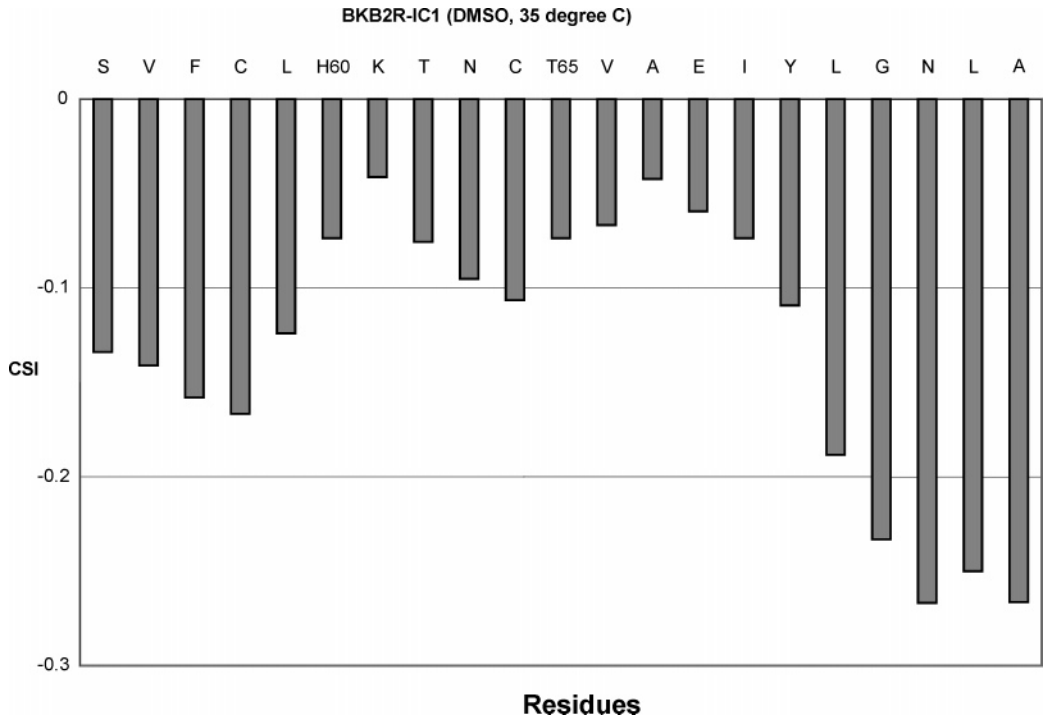

FIGURE 6: Identification of secondary structure in IC1. An NMR plot of the secondary shift, Hα, for the IC1 loop, BKB2R(55−75), of the BKB2R observed in DMSO at 35 °C.

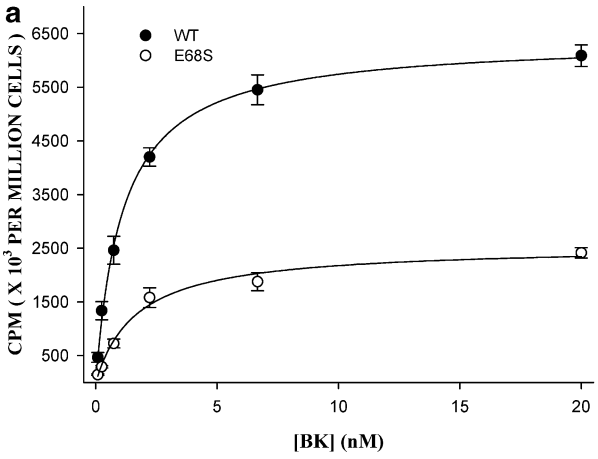

	Kd (nM)	Bmax (X 10^3 receptors per cell)
WT B2R	1.1 ± 0.1	54.1 ± 1.5
E68S	1.7 ± 0.3	21.6 ± 1.1

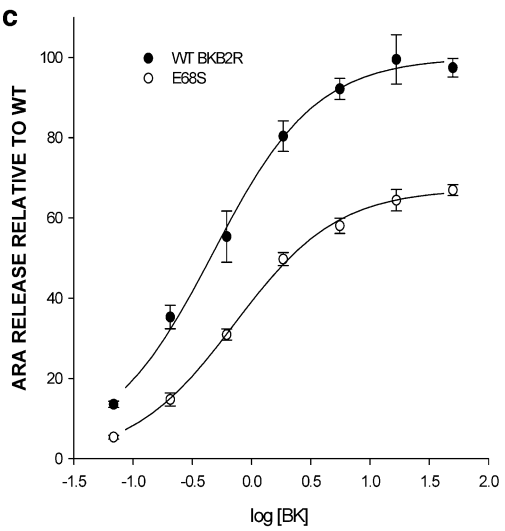

	EC50 (nM)	Emax (% of WT Emax)
WT B2R	0.5 ± 0.1	100 ± 2.1
E68S	0.7 ± 0.1	67.3 ± 2.0

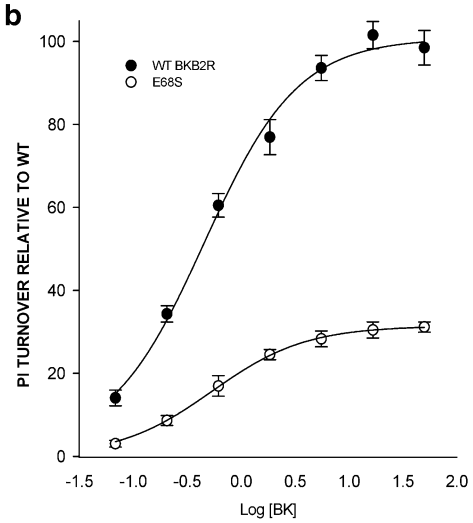

	EC50 (nM)	Emax (% of WT Emax)
WT B2R	0.5 ± 0.1	100.0 ± 2.1
E68S	0.5 ± 0.2	31.4 ± 1.1

FIGURE 7: Mutagenesis studies on E68. (a) Ligand binding of mutant E68S. E68 of wild-type BKB2R was mutated to S. Experimental procedures were the same as those described in Figure 1b. (b) Concentration−response curve of BK-stimulated inositol phosphate production. Experimental procedures were the same as those described in Figure 1c. (c) Concentration−response curve of BK-stimulated ARA release. Experimental procedures were the same as those described in Figure 1d.

Quitterer and co-workers used site-directed antibodies against the IC1 to investigate its location. Their results suggested an extracellular orientation of the IC1 (*23*). There has been no followup report confirming or negating this new BKB2R topology. Here, we illustrate that the IC1 influences receptor folding which may in turn affect ligand binding. Furthermore, we find that role can be assigned to specific amino acids and that pairwise interactions are taking place within the BKB2R IC1.

When six residues of BKB2R IC1 (HKTNCT, based on the rhodopsin crystal structure) were replaced with the corresponding residues of AT1aR IC1 (YMKLKT), the chimera showed very low ligand binding and lost BK stimulated PI turnover and arachidonic acid release most likely due to the binding deficiency. This observation is unlike that found with other chimeric exchanges such as those in the proximal region of the C-terminus where a motif, KSRE, proved crucial to BKB2R signal function but did not have a major effect on ligand binding (*17*). Unchanged binding data were also observed with respect to mutations within the IC2 and IC3 (*7*, *18*). In the present study, the binding became defective and was likely responsible for the subsequent poor signaling functions. The possible reason(s) for defective ligand binding could be a lack of receptor trafficking and/or insertion into the plasma membrane or defective ligand binding of an inserted receptor. Results using anti-FLAG ELISA showed that the poorly binding receptors are expressed on the cell surface. In fact, the level of

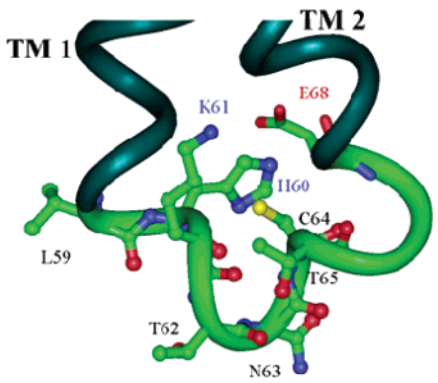

FIGURE 8: Molecular modeling. Structural features of the IC1 of BKB2R. The structure of IC1 superimposed onto the TM helices of BKB2R. The helices, as defined by NMR and molecular modeling, are shown in dark green. The IC1 is shown in light green, with the side chains depicted in ball and stick (nitrogen, blue; oxygen, red; sulfur, yellow). The side chain of E68 (depicted as sticks) is shown projecting toward the IC1, interacting with positively charged residues.

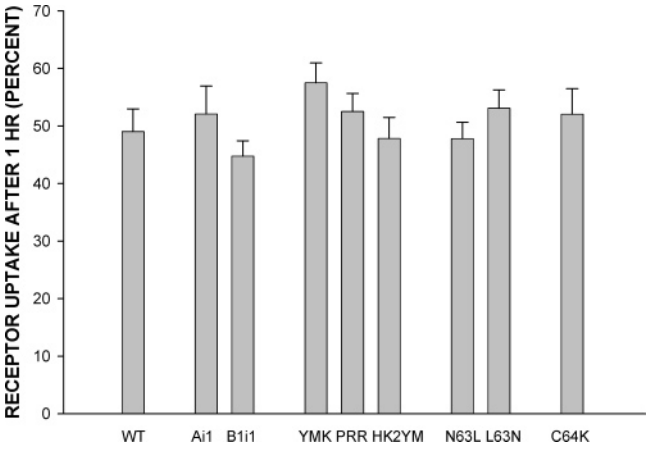

FIGURE 9: Receptor internalization of BKB2R first intracellular loop exchanges with AT1aR and BKB1R segments. Cells were incubated with 100 nM BK for 60 min. After acid stripping and three washes with ice-cold buffer, [^{3}H]BK binding to Rat-1 cells was measured as described in Materials and Methods. Results represent the percentage of receptors internalized in 60 min as compared to receptors internalized in 0 min. Values are the mean ± SE from two to three experiments in triplicate. Using a $p = 0.01$ value as the standard, none of these exchanges affected endocytosis compared to WT BKB2R.

membrane insertion in case of the totally substituted BKB2R IC1 with the AT1aR IC1 (Ai1) proved identical to that of the WT BKB2R. We attempted to calculate the K_d of the binding of the Ai1 mutant, but it is not determinable from nonlinear regression curve fit by the SigmaPlot program because of the low binding. Since a high enough specific activity of ^{3}H-labeled BK is not available, we measured PI turnover with a very high concentration of cold BK. No PI turnover up to 5 μM BK was evident, which suggests that a shift in K_d for the binding of BK to the mutant Ai1 receptor is not taking place. At this time the role of the IC1 in ligand binding is not clear. Our results point to an inappropriate tertiary conformation of the mutated receptor as the reason for the very low binding. Interestingly, Quitterer and co-workers used site-directed antibodies to investigate the topological arrangement of the BKB2R and proposed that the BKB2R IC1 was extracellular (*23*). To date, such a topological arrangement has not been reported for any other GPCR. Thus, no further speculation as to the IC1 participation in BK binding within the extracellular binding pocket can be made at this time.

To determine whether the results with the IC1 are unique to exchanges between BKB2R and AT1aR, the IC1 of BKB1R (a bradykinin receptor subtype) was selected as another IC1 donor for further chimeric studies. BKB1R, whose six amino acid sequence within the IC1 is totally different from that of BKB2R, turned out to bind bradykinin at about the same level as WT BKB2R. This mutant also mediated PI turnover and ARA release to the same level as WT BKB2R. The bradykinin binding data of smaller chimeric receptors, where only the N-terminal three residues (HKT) were replaced with AT1aR (YMK) and BKB1R (PRR), were shown to be similar to WT BKB2R. Both chimeras also showed normal PI turnover and arachidonic acid release as WT. The N-terminal portion of all AT1a, BKB2, and BKB1 receptors contains at least one positive residue. And, in fact, our experiments illustrate that at least one positive residue is necessary in this region of the BKB2R for ligand binding. This was exemplified by the HK2YM mutant which lacked positive charge in this motif and also bound BK very poorly.

With T65 (the last residue in BKB2R IC1) conserved in AT1aR, the importance of the two remaining N63 and C64 within the C-terminal IC1 was next determined. Using the chimera Ai1 as the starting construct, we attempted to rescue ligand binding by changing L63 back to N or K64 back to C. K64 to C proved unable to recover the binding. The L63 to N exchange resulted in a receptor binding BK comparable to WT BKB2R. In this case, the PI turnover and ARA release were also recovered to WT levels. These results illustrate the importance of N63 for the appropriate binding of BK to BKB2R. Interestingly, within the realm of the BKB1 or BKB2 receptors, there are no hydrophobic residues at position 63. However, N is unique to the rat BKB2R. Most of BKB2 receptors from other species contain serine in this position. Serine is also hydrophilic. Rat BKB1R contains a Q, and other BKB1Rs contain either S or R (*24*). This suggests that in the BKB2R and BKB1R a residue with a hydrophilic side chain is preferable in this position. However, a hydrophobic residue (Leu) in this position disrupts ligand binding. Although it would be exciting to speculate on the importance of this position within the IC1 in GPCRs other than BKB2R and BKB1R, at this time no further conclusion should be drawn beyond these two receptors because extensive residue variability exists in other GPCRs not only with respect to the given residue but also with respect to residue hydrophobicity (*24*). Molecular modeling of the BKB2R indicates that N63 is located at the apex of the IC1, projecting toward the solvent (Figure 8). Replacement of N63 with a hydrophobic residue (e.g., N63L) causes the loop to be closely associated with the plasma membrane. This is exemplified by an embedding of the hydrophobic leucine into the decane layer which was used in the simulations. X-ray crystallography of bovine rhodopsin exhibits a rigid organization around the IC1 (*16*). Therefore, one possible mechanism is that by altering the structure of the IC1, the topological arrangement of the adjacent TM helices (TM1 and TM2) is disturbed, thereby affecting ligand binding on the extracellular portion of the receptor.

Initially the IC1 region of the BKB2R was assigned on the basis of the crystal structure of bovine rhodopsin (*16*). To determine a more definitive structure of the BKB2R IC1 experimentally, NMR studies were performed. These NMR studies illustrated that the IC1 of the BKB2R does not concur entirely with that predicted from the crystal structure of bovine rhodopsin. The IC1 starts at H60, in accord with the rhodopsin model; however, the BKB2R IC1 ends at I69 instead of T65. Therefore, the NMR data assign E68 to the IC1 region. Interestingly, the computer prediction of the GPCR topology based on hydrophobicity, charge bias, helix lengths, and geometrical constraints at the Swiss-Prot Database also indicates that E68 is located in the IC1 region (*24*). E68 is highly conserved in the family of BK receptors; on the other hand, the AT1 receptors from various species contain a serine in this location. The single point mutant, E68S, in WT BKB2R reduced ligand binding by more than 60%, suggesting the importance of this negatively charged residue in the tertiary structure of the receptor. In fact, modeling data demonstrate a close proximity of this E68 and the positively charged residues (H60, K61) located in the N-terminal IC1 (Figure 9). Coulombic attraction appears to be an additional important stabilizing force, determining the local IC1 structure, which in turn influences the orientation of TM helices and ultimately ligand binding within the extracellular binding pocket. Interestingly, the BKB1R has two positive residues in the N-terminal portion of its IC1; it also contains an E in the same position as the BKB2R. And, indeed, the BKB2R chimera in which the IC1 of BKB2R is swapped with that of the BKB1R binds BK and signals as WT BKB2R.

The role of the BKB2R C-terminal tail in receptor internalization has been studied extensively (*3*, *7*, *9*−*11*). However, there is little information on the role of the IC1 in receptor uptake. Using $p = 0.01$ values as the cutoff point, the present results show that all of the IC1 mutants tested internalized to about the same extent as WT BKB2R. These results strongly suggest that the first intracellular loop does not participate in the endocytosis of the BKB2R.

In summary, the structural and functional investigation presented here, targeting the IC1 of the BKB2R, provides new insights into the molecular conformation of this region. Our results illustrate that E68 is located in the IC1 of BKB2R. Within this region, the Coulombic interactions among H60, K61, E68, and the cytoplasm-oriented position of N63 are vital for appropriate receptor tertiary structure, ligand binding, and receptor signaling. These results, coupled with our chimeric studies on other receptor regions (*4*, *13*, *17*, *18*), provide evidence that within the cytosolic face of the BKB2R certain motifs are irreplaceable not only for signal transduction but also with respect to determining the tertiary structure of the receptor important in its binding of ligand.

REFERENCES

1. Sharma, J. N. (2003) Does the kinin system mediate in cardiovascular abnormalities? An overview, *J. Clin. Pharmacol. 43*, 1187−1195.
2. Liebmann, C. (2001) Bradykinin signalling to MAP kinase: cell-specific connections versus principle mitogenic pathways, *Biol. Chem. 382*, 49−55.
3. Prado, G. N., Taylor, L., Zhou, X., Ricupero, D., Mierke, D. F., and Polgar, P. (2002) Mechanisms regulating the expression, self-maintenance, and signaling-function of the bradykinin B2 and B1 receptors, *J. Cell. Physiol. 193*, 275−286.
4. Kaplan, A. P., Joseph, K., and Silverberg, M. (2002) Pathways for bradykinin formation and inflammatory disease, *J. Allergy Clin. Immunol. 109*, 195−209.
5. Yu, J., Prado, G. N., Taylor, L., Pal-Ghosh, R., and Polgar, P. (2002) Hybrid formation between the intracellular faces of the bradykinin B2 and angiotensin II AT1 receptors and signal transduction, *Int. Immunopharmacol. 2*, 1807−1822.
6. Marceau, F., and Bachvarov, D. R. (1998) Kinin receptors, *Clin. Rev. Allergy Immunol. 16*, 385−401.
7. Yu, J., Prado, G. N., Taylor, L., Piserchio, A., Gupta, A., Mierke, D. F., and Polgar, P. (2002) Global chimeric exchanges within the intracellular face of the bradykinin B2 receptor with corresponding angiotensin II type Ia receptor regions: generation of fully functional hybrids showing characteristic signaling of the AT1a receptor, *J. Cell. Biochem. 85*, 809−819.
8. Zhou, X., Prado, G. N., Taylor, L., Yang, X., and Polgar, P. (2000) Regulation of inducible bradykinin B1 receptor gene expression through absence of internalization and resensitization, *J. Cell. Biochem. 78*, 351−362.
9. Prado, G. N., Mierke, D. F., Pellegrini, M., Taylor, L., and Polgar, P. (1998) Motif mutation of bradykinin B2 receptor second intracellular loop and proximal C terminus is critical for signal transduction, internalization, and resensitization, *J. Biol. Chem. 273*, 33548−33555.
10. Prado, G. N., Taylor, L., and Polgar, P. (1997) Effects of intracellular tyrosine residue mutation and carboxyl terminus truncation on signal transduction and internalization of the rat bradykinin B2 receptor, *J. Biol. Chem. 272*, 14638−14642.
11. Piserchio, A., Prado, G. N., Zhang, R., Yu, J., Taylor, L., Polgar, P., and Mierke, D. F. (2002) Structural insight into the role of the second intracellular loop of the bradykinin 2 receptor in signaling and internalization, *Biopolymers 63*, 239−246.
12. Wishart, D. S., Sykes, B. D., and Richards, F. M. (1992) The chemical shift index: a fast and simple method for the assignment of protein secondary structure through NMR spectroscopy, *Biochemistry 31*, 1647−1651.
13. Prado, G. N., Mierke, D. F., LeBlanc, T., Manseau, M., Taylor, L., Yu, J., Zhang, R., Pal-Ghosh, R., and Polgar, P. (2001) Role of hydroxyl containing residues in the intracellular region of rat bradykinin B(2) receptor in signal transduction, receptor internalization, and resensitization, *J. Cell. Biochem. 83*, 435−447.
14. Berendsen, H. J. C., van der Spoel, D., and van Drunen, R. (1995) GROMACS: A message-passing parallel molecular dynamics implementation, *Comput. Phys. Commun. 91*, 43−56.
15. Lindahl, E., Hess, B., and van der Spoel, D. (2001) GROMACS 3.0: A package for molecular simulation and trajectory analysis, *J. Mol. Model. 7*, 306−317.
16. Palczewski, K., Kumasaka, T., Hori, T., Behnke, C. A., Motoshima, H., Fox, B. A., Le Trong, I., Teller, D. C., Okada, T., Stenkamp, R. E., Yamamoto, M., and Miyano, M. (2000) Crystal structure of rhodopsin: A G protein-coupled receptor, *Science 289*, 739−745.
17. Yu, J., Liu, B., Eramian, D., Mierke, D., Taylor, L., and Polgar, P. (2004) K317, R319, and E320 within the proximal C-terminus of the bradykinin B2 receptor form a motif important for phospholipase C and phospholipase A2 but not connective tissue growth factor related signaling, *J. Cell. Biochem. 92*, 547−559.
18. Pal-Ghosh, R., Yu, J., Prado, G. N., Taylor, L., Mierke, D. F., and Polgar, P. (2003) Chimeric exchanges within the bradykinin B2 receptor intracellular face with the prostaglandin EP2 receptor as the donor: importance of the second intracellular loop for cAMP synthesis, *Arch. Biochem. Biophys. 415*, 54−62.
19. Wu, V., Yang, M., McRoberts, J. A., Ren, J., Seensalu, R., Zeng, N., Dagrag, M., Birnbaumer, M., and Walsh, J. H. (1997) First intracellular loop of the human cholecystokinin-A receptor is essential for cyclic AMP signaling in transfected HEK-293 cells, *J. Biol. Chem. 272*, 9037−9042.
20. Wu, S. V., Yang, M., Avedian, D., Birnbaumer, M., and Walsh, J. H. (1999) Single amino acid substitution of serine82 to asparagine in first intracellular loop of human cholecystokinin (CCK)-B receptor confers full cyclic AMP responses to CCK and gastrin, *Mol. Pharmacol. 55*, 795−803.

21. Arora, K. K., Krsmanovic, L. Z., Mores, N., O'Farrell, H., and Catt, K. J. (1998) Mediation of cyclic AMP signaling by the first intracellular loop of the gonadotropin-releasing hormone receptor, *J. Biol. Chem. 273*, 25581−25586.
22. Min, K. C., Zvyaga, T. A., Cypess, A. M., and Sakmar, T. P. (1993) Characterization of mutant rhodopsins responsible for autosomal dominant retinitis pigmentosa. Mutations on the cytoplasmic surface affect transducin activation, *J. Biol. Chem. 268*, 9400−9404.
23. Quitterer, U., Zaki, E., and AbdAlla, S. (1999) Investigation of the extracellular accessibility of the connecting loop between membrane domains I and II of the bradykinin B2 receptor, *J. Biol. Chem. 274*, 14773−14778.
24. Horn, F., Vriend, G., and Cohen, F. E. (2001) Collecting and harvesting biological data: The GPCRDB & NucleaRDB databases, *Nucleic Acids Res. 29*, 346−349.

BI048288I